THE ASTROPHYSICAL JOURNAL, 424:76–83, 1994 March 20

INTERMEDIATE-RESOLUTION SPECTROPOLARIMETRY OF A SMALL SAMPLE OF QUASARS

J. A. DE DIEGO, M. R. KIDGER, AND E. PÉREZ
Instituto de Astrofísica de Canarias, E-38200 La Laguna, Tenerife, Spain
AND
L. O. TAKALO
Tuorla Observatory, Tuorla, SF-21500 Piikkiö, Finland
Received 1993 June 14; accepted 1993 September 22

ABSTRACT

We present spectropolarimetric observations of a sample of three quasars selected because of their very different broad-band polarization properties. All of the objects in the sample show frequency-dependent polarization degree (FDP), and two of them also show frequency-dependent polarization position angle (FDPA). We have not detected polarization in the spectral emission lines in any object of the sample, although the possibility exists that the iron blends in CTA 102 may be polarized. Our observations show important differences between the three objects. While 3C 273 has been previously discussed in terms of a multiple synchrotron source model, a conclusion supported by our results, this seems not to be the case for 3C 345. We examine a number of processes capable of generating the observed FDP and FDPA of this object. A combination of a nonthermal source and scattering from dust or gas in the local interstellar medium can explain our observations, although some restrictions must be imposed to avoid polarization of the spectral emission lines. The quasar CTA 102 shows a very complex wavelength-dependent polarization, which may be related to the iron blends in the spectrum. We also present a statistical test developed by us to examine the possible polarization of the lines.

Subject headings: galaxies: nuclei — polarization — quasars: general

1. INTRODUCTION

In the last decade, various groups have made interesting spectropolarimetric studies of active galactic nuclei (AGNs). Given the knowledge that their continuum is usually polarized (although at a low level of under 1%), these studies have tried to determine if the spectral emission lines are also polarized. Due to a lack of appropriate instruments, the research has focused mainly on bright Seyfert 2 and radio galaxies (e.g., McLean et al. 1983; Miller & Antonucci 1983; Antonucci & Miller 1985; Goodrich 1989a, b; Antonucci 1992; Jackson 1992; Cimatti et al. 1993) and much less on quasars (Goodrich & Miller 1988). The discovery by Antonucci & Miller (1985) that the Seyfert 2 galaxy NGC 1068 looks like a Seyfert 1 when observed in polarized light led to the development of the unified model for Seyferts. Since then, Miller & Goodrich (1990) have found at least four other Seyfert 1 galaxies hidden in Seyfert 2 galaxies. These observations have led to the model with a thick torus of obscuring material within the narrow-line region, which extended beyond the broad-line region. In such a model, the appearance of the galaxy as a Seyfert 1 or 2 is explained by its relative orientation to the observer. In general, the results of these studies have shown that the emission lines are usually polarized, although they do not always share the polarization of the continuum. Electron scattering has been proposed as the polarization mechanism of the emission lines. Spectropolarimetry of a sample of radio galaxies by Cimatti et al. (1993) and by Jackson & Tadhunter (1993) shows a polarized blue continuum, which may be explained as a scattered continuum from the nucleus.

Blazars are AGNs with both high polarization and high amplitude, fast variability, both in flux and in polarization, with this variability extending over the whole electromagnetic spectrum, from radio to X-rays. Many observations have shown that frequency-dependent polarization degree and position angle are common in blazars. However, not all the sources present this phenomenon, and those which present it do so only intermittently (e.g, Takalo et al. 1992b); the frequency-dependent polarization degree (FDP), when present, may change or even vanish from one night to the next (Kidger et al. 1993). Several models have been proposed to explain these phenomena, such as multiple synchrotron sources (e.g., Valtaoja et al. 1991) or geometrical effects (Björnsson 1985). In § 4 we will briefly review these models and their ability to explain our observations.

In de Diego et al. (1992, hereafter Paper I) we discussed the spectropolarimetric observations of 3C 273. The conclusions of our study were that the emission lines of this quasar presented no detectable polarization and that the polarization could be understood as the result of a multiple synchrotron source, in accordance with the hypothesis expressed by Impey, Malkan, & Tapia (1989) and Valtaoja et al. (1991).

In this paper, we present the results of the other two objects of our sample, as well as some additional comments on the observations of 3C 273. The sample consists of 3C 273, which is a low-polarization quasar (polarization degree less than 3%), CTA 102, an optically violent variable quasar (OVV), and 3C 345, a blazar. The low-polarization quasar 3C 273 has a redshift $z = 0.158$ and shows both variability in flux and polarization (e.g., Valtaoja et al. 1991; Courvoisier et al. 1988). This activity has been termed *miniblazar* by Impey et al. (1989) and can be explained if a blazar nucleus supplies $\approx 10\%$ of the total flux. The OVV quasar CTA 102 has a high polarization ($> 3\%$), and a redshift $z = 1.037$. The third object, 3C 345, is a blazar with $z = 0.595$, has large and highly variable polarization, and shows OVV activity and variability on all timescales from a few minutes to more than 10 yr. It is also one of the

most observed blazars, and it has been monitored by our group with optical and infrared photometry and optical polarimetry over many years (e.g., Kidger et al. 1993, who present data for the 1992 outburst). At the time that it was observed, 3C 345 was passing through a sustained outburst (Takalo et al. 1992a; Kidger et al. 1993; Schramm et al. 1993) and had $V = 16.8$. We also present, in the Appendix, a detailed description of the statistical reduction procedure used to analyze the data.

2. OBSERVATIONS AND REDUCTION

The observations were taken with the 4.2 m William Herschel Telescope located in the Spanish observatory of El Roque de Los Muchachos, on the island of La Palma, on 1991 June 11–12. We used the Faint Object Spectrograph with a blue-sensitive GEC (EEV) coated chip, with a resolution of approximately 4 Å in the blue and 8 Å in the red. The blue part of the spectrum is measured in the second-order spectrum of the incoming light. To calculate the Stokes parameters for the linear polarization, it is necessary to perform four exposures of each object. We made 4 × 300 s exposures for 3C 273 and 4 × 1200 s exposures for both CTA 102 and 3C 345. A more complete discussion of the instrument and the calibration of the observations can be found in Paper I. In order to perform a spectropolarimetric analysis, it is necessary to get a rather high signal-noise ratio, 500 in each of the four exposures for an error in the Stokes parameters of 0.1%, which corresponds to the detection of 10^6 photons. The precision of the measurements is critical in order to distinguish possible small dependences of the polarization with wavelength. Thus, the data were binned in order to reduce the errors to a few tenths of a per cent in the Stokes parameters. Table 1 shows the signal-noise ratio and the Stokes parameter errors of the binned data. The binned data has small errors, while the wavelength resolution is high enough to analyze the behavior of the strong and isolated emission lines (bin size is of the order of 100 Å; its exact value depends on the amount of signal). The possibility remains, if the results justify the effort, of resampling parts of the data in order to obtain a higher wavelength resolution of the emission lines, at the expense of greater errors in the determination of the Stokes parameters.

To determine the polarization of the emission lines, it is possible to fit a polynomial to the Stokes parameters and to test the fit in order to find deviations that suggest possible polarization of the emission lines. Instead of this, we have used a more cumbersome procedure which, nevertheless, has its advantages (see Appendix). First, it allows us to identify at once which parts of the spectrum have a different polarization degree, instead of comparing the fit obtained from two distributions, one for each Stokes Parameter. Second, the test allows an easy check of the errors in our calculations. The latter characteristic has been very useful in the case of CTA 102, because the polarization of this source is so complex that the reader may be tempted, as we were, to think that our error estimate is inadequate. On recalculation, no difference was found, and, as we will see later, our test confirms the accuracy of the estimated errors.

In our method, we calculate the amount of the polarization degree that cannot be explained by the continuum polarization, as well as the estimated error for that noncontinuum polarization. We will refer to this derived polarization as *residual* polarization. For the reasons discussed in the Appendix, for an object in which the polarization emission is produced only by its continuum component, the expected distribution of the residual polarization is statistically similar to the distribution of the residual polarization errors. Thus, comparing the actual distribution of the residual polarization with the distribution of its errors, we check the accuracy of the error estimation of the Stokes parameters and, from those zones in which the two distributions diverge, the possible polarization of the strong and isolated emission lines.

TABLE 1

SIGNAL-TO-NOISE RATIO AND STOKES PARAMETER ERRORS FOR BINNED DATA

Object	Spectral Range	Signal-to-Noise Ratio	Stokes Parameter Errors
3C 273	Blue	300	0.0020
	Red	700	<0.0010
CTA 102	Blue	150	0.0040
	Red	300	0.0020
3C 345	Blue	200	0.0025
	Red	300	0.0010

NOTES.—The blue spectra range from 3450 to 4800 Å in the observed frame, and the red spectra from 4800 to 9800 Å.

3. RESULTS

3.1. 3C 273

The 3C 273 data has been already presented in Paper I. Here we present in Figure 1 only the residual polarization. Looking at Figure 1, we see that none of the calculated residual polarization bins (*solid line*) are more than 2 σ from their expected value (*dotted line*), which also correspond to the bin errors (see Appendix). Hence, as for CTA 102 and 3C 345 (see below), no evidence of polarization was found for the strong and isolated emission lines of 3C 273. As commented on in Paper I, we find that a multiple synchrotron source model (Impey et al. 1989; Valtaoja et al. 1991) gives the best fit to our data.

3.2. CTA 102

The CTA 102 spectrum (Fig. 2), shows the usual emission lines observed in intermediate-redshift quasars, i.e., C III

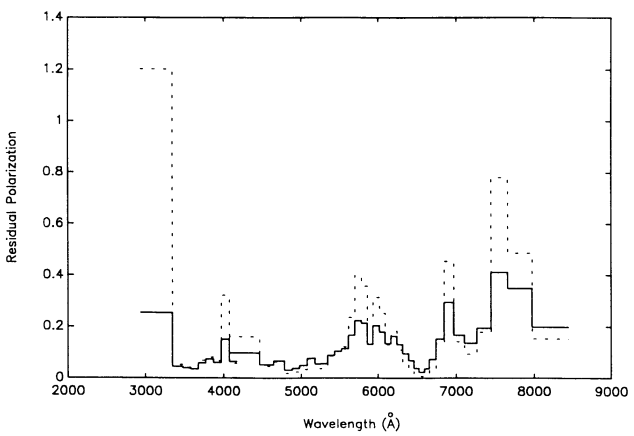

FIG. 1.—Residual polarization degree for 3C 273 resulting from subtracting an estimation of the Stokes parameters of the continuum, to those calculated directly from the observations. The calculated residual polarization is shown as a solid line. The dotted line shows the predicted polarization for a non-polarized source, resulting from measurement errors. Wavelengths refer to the rest frame.

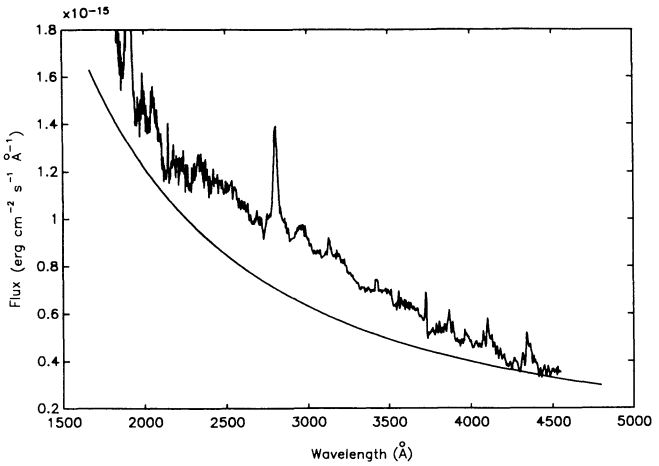

FIG. 2.—CTA 102 spectrum. The line shows the power-law fit to the continuum.

(λ1909), Mg II (λ2798), [Ne V] (λ3426), [O II] (λ3727), [Ne III] (λ3869–3965), Hδ, Hγ, as well as the iron blends between 2200 and 2700 Å, although, in reality, the strong iron blends extend over the whole range of the quasar's spectrum, from the ultraviolet to the infrared.

The polarization degree (Fig. 3), has a complex distribution. A test for variances shows that FDP is present, with a probability greater than 99.5%. A visual comparison of the polarization degree with the theoretical spectrum of Fe II blends appears to show considerable similarity (see Fig. 3 of Wills, Netzer, & Willis 1985), suggesting that the iron blends may make a contribution to the polarization spectrum, particularly between 2000 and 3000 Å. In an attempt to confirm this, we binned the data with different bin sizes, always getting the same result.

At this point it is worth noting that the possible polarization of the Fe II blends in CTA 102 is suggested based on our own perception, but it is not supported by statistical tests. The principal reason which makes us think that the statistical tests for the Fe II blends are inadequate for our data is that our observations were obtained to test strong and isolated spectral lines. Although the integrated contribution of the Fe II blends to the total flux is large, they lie over a rather extended part of the spectrum, which, at our effective resolution, does not allow us to separate their contribution from that of the estimated continuum. Nevertheless, there are a number of coincidences that make us suspect the possible polarization of these blends. The maximum of the polarization in the blue part of the spectrum coincides with the peak of the Fe II blends. Were these blends to be unpolarized, we would expect to find a decrease in the polarization at this wavelength, instead of an increase to $\approx 1.5\%$ in the polarization degree in the range of 2300 to 2600 Å (Fig. 3*a*). It should also be noted that a similar result was obtained by Antonucci & Miller (1985), who observed the polarization of the Fe II blends in NGC 1068. No similar effect can be seen in 3C 345 (our spectrum of 3C 273 starts only at 3000 Å).

We also see that the position angle shows complex variations about a value of 160° (Fig. 3), with a dispersion considerably greater than the errors. A test for variances shows that these variations have a probability greater than 99.5% of being real. The variations of the position angle extend along the whole spectrum with approximately constant amplitude. Hence, these variations are not related with the emission from the Fe II blends, which are significant only in the range from 2300 to 2600 Å. The position angle is not related to the polarization degree either, as shown by a least-squares fitting. The origin of the very complex frequency-dependent polarization position angle (FDPA) in CTA 102 is probably related to a very intricate mixture of effects, which cannot be extracted from our current data.

In order to subtract the continuum to make our test for the polarization of strong and isolated emission line, we fitted a power law, with $\kappa = 1.6$, to the data (see Appendix). The continuum is shown in Figure 2 as the smooth, continuous line.

Figure 4 shows both the residual polarization, computed by the method outlined in the Appendix, and the predicted residual polarization. After performing the statistical test discussed in § 2, we concluded that the smaller, line-sized structures can be explained by the measurement errors. Thus, no strong, resolved line polarization is found to the limit of our observations. Figure 4 also shows that the errors in the polarization degree can account for the calculated residual polarization.

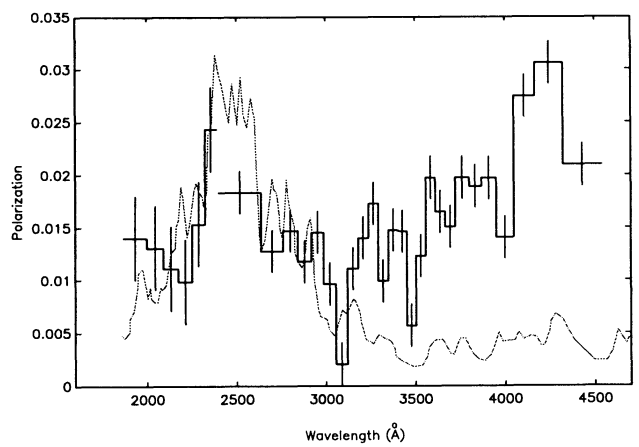

FIG. 3*a*

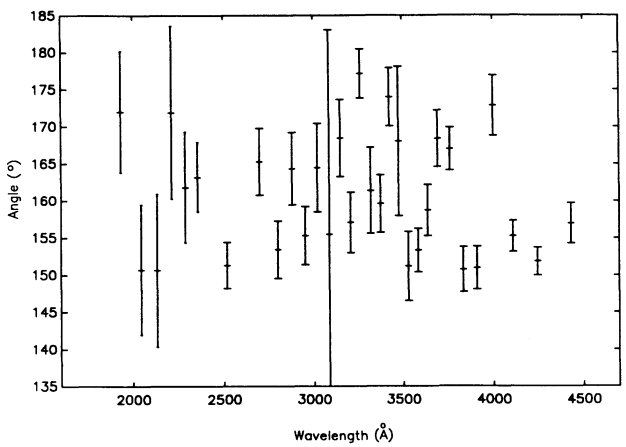

FIG. 3*b*

FIG. 3.—Polarization degree (*a*) and polarization position angle in degrees (*b*) for CTA 102. Wavelengths refer to the rest frame.

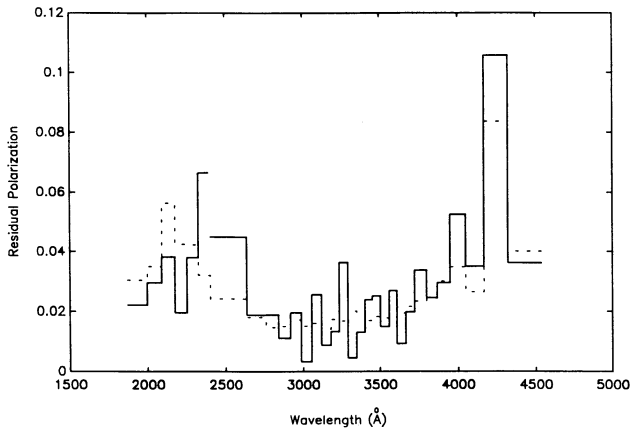

FIG. 4.—Residual polarization degree for CTA 102 resulting from subtracting an estimation of the Stokes parameters of the continuum from those calculated directly from the observations. The calculated residual polarization is shown as a solid line. The dotted line shows the predicted polarization for a nonpolarized source, resulting from measurement errors. Wavelengths refer to the rest frame.

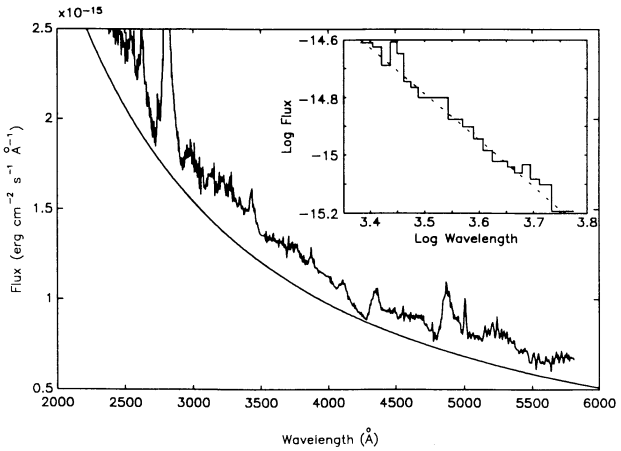

FIG. 5.—Spectrum of 3C 345. The line shows the power-law fit to the continuum. Wavelengths refer to the rest frame. The inset shows the fit of a straight line to the binned spectrum. The units of the inset and the main figure are the same, with the inset plotted on a logarithmic scale.

3.3. 3C 345

Figure 5 shows the spectrum of 3C 345. As in CTA 102, we see the Fe II blends, as well as the Mg II (λ2798), [Ne V] (λ3246), [Ne III] (λ3869), Hδ, Hγ, Hβ emission lines. The continuum can be fitted by a power law with $\kappa = 1.6$. This blazar has a typical polarization degree between 2 and 12%, although a value as high as 36.2% was found during the 1983 outburst (Smith et al. 1986). Previous broad-band polarimetric data obtained with the 2.5 m Nordic Optical Telescope (NOT) show that the wavelength dependence is not usually present (e.g., Kidger et al. 1993). Figure 6 shows that during this observation, the polarization degree of 3C 345 presented a minimum near Mg II, a large increase at 3000 Å, and a minimum at Hβ. None of these features, though, is consistent with the hypothesis that the lines are polarized. Figure 7 shows the residual polarization of 3C 345. As in the cases of 3C 273 and CTA 102, discussed above, the residual, noncontinuum polarization has a distribution that can be explained by the measurement errors, showing no evidence of polarization of the strong and isolated lines.

The position angle recorded in previous observations with the NOT shows either no wavelength dependence or complex wavelength dependence. The position angle shows a peak between 2400 and 3000 Å, along with a net variation of 8° from 3000 to 4000 Å, where it becomes constant.

4. FREQUENCY-DEPENDENT POLARIZATION IN 3C 345

In the previous section, we have found that, to the limit of our observations, the strong and isolated emission lines of the objects in our sample are not polarized, with the possible exception of the iron blends in CTA 102. Nevertheless, the behavior of the polarization degree and position angle of the three objects that we have observed shows that a component other than the assumed nonthermal source must exist in order to account for their wavelength dependence.

We will center our discussion on 3C 345, as it presents the simplest case. The results for 3C 273 were discussed in Paper I and have not been significantly changed by this more detailed

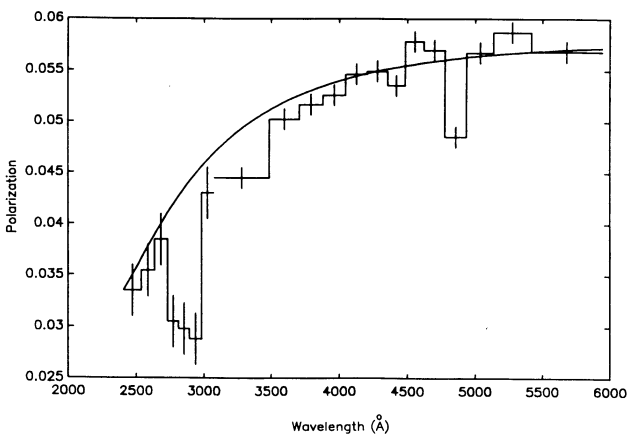

FIG. 6a

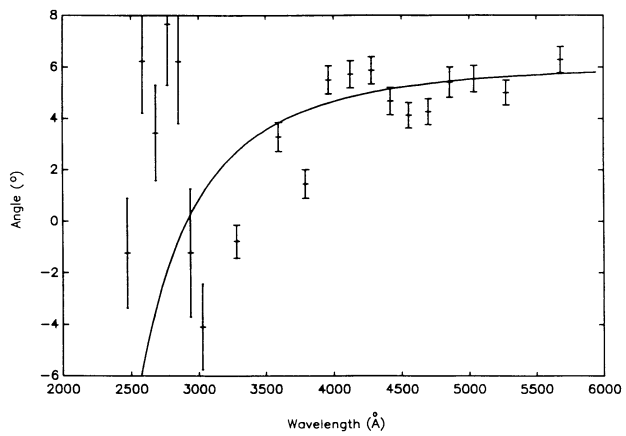

FIG. 6b

FIG. 6.—Polarization degree (*a*) and position angle in degrees (*b*) for 3C 345. The continuous line indicates the polarization degree and position angle resulting from a nonthermal source with wavelength-independent polarization and scattering from gas. Similar results can be obtained by considering dust scattering. Wavelengths refer to the rest frame.

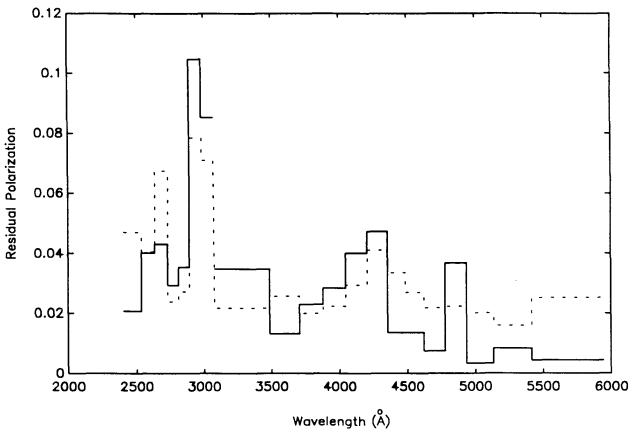

FIG. 7.—Residual polarization degree for 3C 345, resulting from subtracting an estimation of the Stokes parameters for the continuum from those calculated directly from the observations. The calculated residual polarization is shown as a solid line. The dotted line shows the predicted polarization for a nonpolarized source, resulting from measurement errors. Wavelengths refer to the rest frame.

analysis, while CTA 102 presents such a complex behavior that a much better understanding of the processes which take place in the nuclei of quasars is needed before making a suitable model for the results that have been obtained.

There have been many suggestions about the possible origin of the FPD and FDPA angle in blazars; these we will discuss in the context of their ability to fit the observations of 3C 345. Although our own galaxy may affect the observed polarization, as predicted by the Serkowski-Mathewson-Ford law (Serkowski, Mathewson, & Ford 1975), we can neglect its contribution because the galactic latitude of 3C 345 is too large (40°) to have any noticeable influence on the total polarization.

4.1. *Possible Polarization Generation Mechanisms*

First, we will review the possible polarization mechanisms as applied to our observations of 3C 345 and how these mechanisms and other effects can be combined to yield the observed polarization of 3C 345. Finally, we will choose the model that we think can best explain the observations qualitatively and show that it can also fit the observations quantitatively.

Several mechanisms have been proposed for the polarization generation in AGNs. Various of these are implausible and can be rapidly rejected but are included here for completeness and will be dealt with first. Others are more reasonable but are found to be incompatible with the observed polarization behavior. Finally, we find a single model which does not suppose any insurmountable contradictions with the observations presented here.

When the electron distribution is not a power law, different regions in a nonthermal source may make different relative contributions to the total flux. Norsieck (1976) considered several small asymmetries in the electron distriubtion of a synchrotron source, needing a curved spectrum to obtain FDP which, in any case, was always rather small. Björnsson & Blumenthal (1982) related the FDP to a change in the synchrotron source geometry relative to the normal component of the magnetic field, but they saw a tendency of the polarization degree to increase with frequency (Björnsson 1985), exactly the opposite to our observations.

Electron scattering produces wavelength-independent polarization, and the emission lines are expected to share the same polarization as the continuum, unless restrictions are included in the model on the relative placement of the scattering, continuum emission, and line emission regions. A combination of electron scattering and a nonthermal source can also produce FDP and FDPA, but, as the electron scattering is wavelength independent, the dependence of the resulting polarization should be smooth and simple. Although an inhomogeneous scattering medium could produce wavelength-dependent polarization, a very fine tuning is necessary to explain the FDPA between 2500 and 3000 Å.

Wavelength-dependent transmission through a dispersive medium (i.e., Faraday rotation, dust transmission, and dust extinction) can also produce different effects on the observed polarization. Thus, extinction, combined with the nonthermal component, may produce FDP but not FDPA, while Faraday rotation can produce both FDP and FDPA. Although the medium in quasars may have suitable conditions to produce Faraday rotation in the optical (i.e., large magnetic fields and high electron densities, e.g., Brown et al. 1989; Kidger & de Diego 1992), the effect should be more noticeable at longer than at shorter wavelengths, which is not the case of our observations of 3C 345. In fact, Faraday rotation has never been detected at optical wavelengths in quasars, reinforcing the assumption of the nonthermal origin of the continuum. The best explanation is that nonthermal processes need strong magnetic fields, which are normally oriented to the observer, with both the intensity and the polarization degree decreasing sharply when the orientation is different from the normal. Faraday rotation, on the other hand, requires that the magnetic field should be aligned with the observer. The overall result is that whenever there is nonthermal polarization, there cannot be Faraday rotation, and when Faraday rotation might occur, there is no nonthermal polarization.

Dust transmission through a medium composed of aligned grains is capable of producing polarization as well as extinction. However, the Serkowski et al. (1975) law yields a rather smooth FDP compared to the one that is observed in 3C 345, and no FDPA is expected, unless there is a nonuniform alignment, coupled with a change in the dust grain properties along the line of sight (Martin 1974)—in other words, a rather unlikely set of circumstances. As in the cases of dust reflection and electron scattering, some geometrical restriction must be imposed to avoid polarized emission lines.

Dust reflection in an optically thin scattering medium would yield a constant polarization angle and a rapid increase in the polarization degree toward the blue. Instead of this, the polarization degree observed in 3C 345 diminishes to shorter wavelengths, and there is an obvious FDPA. The polarization increase toward the blue would be avoided if there were an optically thick medium (Rudy & Schmidt 1988), where the effective scattering geometry might be wavelength dependent (Martin 1985), resulting in a modified FDP and FDPA, but some additional restrictions are still needed to explain the lack of polarization in the emission lines. On the other hand, dust transmission and extinction, combined with the nonthermal source, may produce FDP, principally from extinction, and also produce FDPA, as the resulting polarization of the nonthermal component is diminished after extinction, but the polarization position angle variations are too large in the range of 2500 to 3000 Å to be explained by a simple combination of two sources.

A similar effect is seen with smaller particles. Atoms, ions, and molecules interact with the radiation field, producing Ray-

leigh scattering. Its signature is a power-law dependence with index -4, and it yields a larger polarization as the scattering angle approaches $\pi/2$. Scattering by larger particles, such as dust, would produce a dependence with a power law with an index greater than -4 and a smaller polarization degree.

Contamination of the polarized radiation by the background galaxy can explain the FDP observed in some blazars, like Markarian 501 (Takalo et al. 1992b), where the background galaxy is easily detected. As the *thermal* emission of the galaxy peaks in the infrared range, the polarization degree would diminish toward longer wavelengths, and no FDPA would be expected. In the case of 3C 345 we note that no underlying galaxy is seen. If the dilution of the polarized radiation is due to the contribution of the blue bump (Smith, Elston, & Balonick 1986), the FDP is inverted, but still there is no FDPA.

Overlap of two or more independent nonthermal components, with different cutoff frequency distributions, can probably be used to explain the observed FDP and FDPA in any object. In 3C 345, it would be easy to explain the coincidence of the minimum in the degree of polarization with the large variations of the position angle. Nevertheless, such a multiple component source would show a curved spectrum in the observed wavelength range, with the spectral index decreasing with frequency, depending of the exact electron distribution of both components. Figure 5 shows that the spectrum of 3C 345 is well fitted by a straight line (correlation coefficient -0.9869). Thus, no curvature of the spectrum is found either in our data or in many observations of other sources by different observers (see Cruz-Gonzalez & Huchra 1984; Puschell et al. 1983), although some other objects do show curved spectra, e.g., AO 0235+164 or BL Lac. These different results imply that the multiple component model should be used with some caution.

From the different polarization mechanisms discussed above, we see that none of them can explain our observations on their own. Moreover, except when at least one nonthermal source is included, they cannot explain the known polarization variability of 3C 345 either.

Finally, we have also considered a model based on scattering by dust or gas, combined with the nonthermal component, which may produce the observed FDP, although geometrical restrictions have to be imposed to explain the lack of polarization of the emission lines. Scattering by dust or small particles produces a polarization degree which increases to smaller wavelengths. Nevertheless, the effect may be hidden by the polarization of the nonthermal component, which is wavelength independent, resulting in a decrease in the total polarization toward the blue, at least over a limited range of wavelengths, and a change in the resulting polarization position angle. The position angle variations in the range from 2500 to 3000 Å may be due to an optically thick region seen at these wavelengths, occulting the scattering region. Identifying the optically thick region with that responsible for the emission of the Mg II line explains the simultaneous decrease of the polarization degree by dilution.

4.2. *Comparison between Our Adopted Model and the Observations*

We think that the last model is qualitatively the most suitable to account for our observations of 3C 345 because it is the one which provides the simplest initial conditions. It is valid to ask if the model can also explain the observations quantitatively. From Figure 6, we can suggest the existence of a nonthermal component, with both a wavelength-independent polarization degree of 5.8%, normalized to the total flux, and a wavelength-independent polarization position angle of 6°. Thus, adjusting the residual Stokes parameters such that, when they are added to those of the nonthermal radiation, we obtain the observed total Stokes parameters $Q_{\rm obs}$ and $U_{\rm obs}$:

$$Q_{\rm obs} = Q_{\rm nth} + Q_{\rm res} ,$$

$$U_{\rm obs} = U_{\rm nth} + U_{\rm res} ,$$

where the subscripts "nth" and "res" refer to the nonthermal and the residual component, respectively. We find that several functions may fit these residual Stokes parameters. In particular, any power law of the form $S \propto \lambda^p$ may fit, where S is one of the Stokes parameters (Q or U), and $-4 \leq p \leq -2$. In order to show how such a power law can be used to model the observations, we have used $p = -4$. The polarization position angle of this residual polarization is $-67^\circ.5$, and the residual polarization degree, normalized to the total flux, is plotted in Figure 8.

The curves in Figure 6 show how the model fits the observations. Similar results can be obtained throughout the range of values of p. The regions in which the model is most unlike the observed FDP coincide with the position of low-polarization lines (Mg II, Fe II, the Balmer continuum, Hβ). In these regions, the polarization degree is always below the value predicted by the model, which confirms that these emission lines are not polarized. There is also disagreement between the FDPA and the position of the Mg II line. The difference between the predicted and the observed values of the FDP can be understood by contamination of the polarized flux by the lines—basically, the same effect as galactic dilution, but on an smaller scale. As the polarization position angle returns to its usual value of 6° at the position of the Mg II, a further restriction is needed to allow a smaller contribution of the polarized scattered light. If this restriction is of the geometrical kind, a major part of the scattering region responsible for the polarization would be occulted by a region that is optically thick in the range of 2500 to 3000 Å, while the nonthermal continuum would be not hidden. The optically thick region can probably be identified with the region which emits the Mg II line.

The above discussion shows how a combination of a nonthermal source and atomic, or dust scattering, can be modeled to fit our observations of 3C 345. In this context, it is necessary

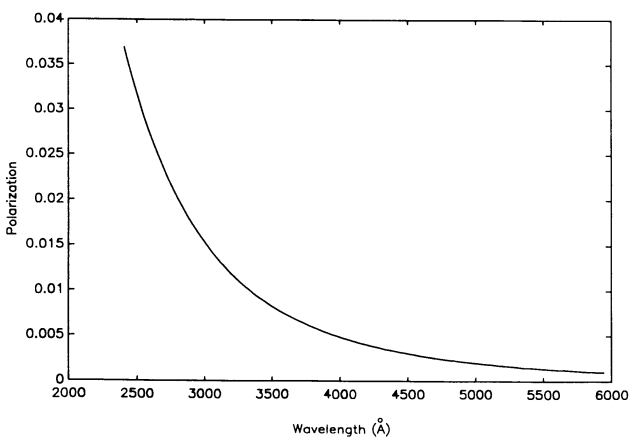

FIG. 8.—Residual polarization of 3C 345, normalized to the total flux. Wavelengths refer to the rest frame.

to argue that the lack of polarization in the emission lines is due to the relative positions of the continuum emitting region, the broad line region, and the scatterers. Apart from the ability of the model to explain these particular observations, it also explains the lack FDP and FDPA during outburst. Kidger et al. (1993) observed 3C 345 during the 1992 outburst, finding neither FDP nor FDPA. This is a logical consequence of the nonthermal source and scattering model. During the outburst, the nonthermal emission rises and the scattered component makes a smaller contribution to the total flux. The relative contribution of the nonthermal component to the total polarization is then enhanced, the total polarization being greater than in quiescence and the position angle constant, as expected from a nonthermal source.

5. CONCLUSIONS

We have presented optical spectropolarimetric observations of the OVV object, CTA 102, and the blazar, 3C 345, as well as some additional comments to our previous paper about spectropolarimetry of the quasar 3C 273. In all three objects of our sample, the polarization degree shows a frequency dependence. CTA 102 and 3C 345 also present a clear frequency dependence of the polarization position angle. In none of the objects have we detected clear evidence of polarized emission lines. The polarization properties of CTA 102 are very complex, probably as a result of the many processes that may be taking place in the nuclei of active galaxies. The relationship between these processes might explain the different polarization properties from one source to another, and even in the same object, and also explain the amazing variability behavior that they often present. The possibility exists that the Fe II blends of CTA 102 present polarization, as was previously detected in NGC 1068 by Antonucci & Miller (1985). Our conclusion in Paper I, where we found that the observations of 3C 273 could be explained by a multiple synchrotron source, cannot be applied directly to CTA 102 and 3C 345, either due to the complexity of the behavior of the data, in the case of CTA 102, or to the lack of spectral curvature, in 3C 345.

We have discussed the ability of these processes to explain the observations of 3C 345 and found that a combination of a nonthermal polarized component, with scattering by dust or gas, is an appropriate interpretation, although it is necessary to argue for geometrical restrictions, in order to avoid polarization of the emission lines. This model also accounts for the polarization observed during the outburst of 3C 345 in April 1992 by Kidger et al. (1993). Other model, such as a combination of the nonthermal source with other processes, especially electron scattering in an inhomogeneous medium, cannot be ruled out, but they need several further restrictions to fit the observational data.

The William Herschel Telescope is operated on the island of La Palma by the Royal Greenwich observatory in the Spanish Observatorio del Roque de Los Muchachos of the Instituto de Astrofísica de Canarias. We wish to thank René Rutten for his helpful discussions in reduction and analysis of data, Jorge Sánchez for useful discussion, and Gabriel Gómez for helping us with the use of the FOS package, kindly made available by J. Allington-Smith. We would also like to thank Chris Impey for his helpful comments about the first version of this manuscript.

APPENDIX

In order to perform the test, we estimate the flux of the continuum adjusting a power law of the form

$$I_{\rm cont} = R\lambda^{\kappa}$$

to the spectrum (the relation between κ and the spectral index α given by $I_{\rm cont} \propto \nu^{-\alpha}$ is $\alpha = \kappa + 2$). We then made an estimate of the Stokes parameters for the continuum. To perform this estimate, we fitted a polynomial of first or second degree. This yields Stokes parameters ($Q_{\rm adj}$ and $U_{\rm adj}$) normalized to the observed flux. To normalize the Stokes parameters to the continuum flux, we multiplied by the observed flux and divided by the estimated continuum flux. We then computed the residual Stokes parameters Q and U as

$$X_{\rm res} = \frac{X_{\rm obs} I_{\rm obs} - X_{\rm cont} I_{\rm cont}}{I_{\rm obs} - I_{\rm cont}},$$

where X can be either Q or U.

The residual Stokes parameters error is computed from

$$\sigma(X_{\rm res})^2 = \left[\frac{\partial X_{\rm res}}{\partial X_{\rm obs}}\sigma(X_{\rm obs})\right]^2 + \left[\frac{\partial X_{\rm res}}{\partial I_{\rm obs}}\sigma(I_{\rm obs})\right]^2 + \left[\frac{\partial X_{\rm res}}{\partial X_{\rm cont}}\sigma(X_{\rm cont})\right]^2 + \left[\frac{\partial X_{\rm res}}{\partial I_{\rm cont}}\sigma(I_{\rm cont})\right]^2.$$

The error $\sigma(X_{\rm cont})$ can be computed as

$$\sigma(X_{\rm cont})^2 = \left[\frac{\partial X_{\rm cont}}{\partial X_{\rm obs}}\sigma(X_{\rm obs})\right]^2 + \left[\frac{\partial X_{\rm cont}}{\partial X_{\rm adj}}\sigma(X_{\rm adj})\right]^2 + \left[\frac{\partial X_{\rm cont}}{\partial I_{\rm obs}}\sigma(I_{\rm obs})\right]^2 + \left[\frac{\partial X_{\rm cont}}{\partial I_{\rm cont}}\sigma(I_{\rm cont})\right]^2,$$

where $\sigma(X_{\rm adj})$ is estimated from the standard deviation of $(X_{\rm obs} - X_{\rm adj})$. As the constant, R, in the estimate of $I_{\rm cont}$ is subjective (it can be explained as being a zero point of the spectrum), it is also the main source or error in the estimation of $I_{\rm cont}$ (κ has a more objective and precise determination). The error, $\sigma(I_{\rm cont})$, may be computed then as

$$\sigma(I_{\rm cont}) \approx \sigma(R)e^{R}\lambda^{\kappa},$$

where we have estimated $\sigma(R) \approx 0.05$.

Finally, the residual polarization error is computed as

$$\sigma_p = \sqrt{\left(\frac{Q}{P}\,\sigma_Q\right)^2 + \left(\frac{U}{P}\,\sigma_U\right)^2}\,.$$

If the continuum were the only source of polarization, the residual polarization would be zero. But as the polarization cannot be negative, this residual will always be positive. We have to compare this residual polarization with the expected polarization resulting from error measurements of a zero polarization source. This zero polarization source would yield a nonzero polarization measurement with a distribution identical to the errors in the measurement of the residual polarization. So the expected polarization is $P_{\rm exp} = \sigma(P_{\rm res})$. Hence, we make an upper-tail χ^2 test to compare the $P_{\rm res}$ and $P_{\rm exp}$ distributions. If they are similar, then we conclude that the only source of polarization (at our resolution) is the continuum. The test is upper-tailed because we are only interested if $P_{\rm res}$ is greater than $P_{\rm exp}$. At this point, we must point out that this part of the test should give always the same result, i.e., no evidence that $P_{\rm res} \neq P_{\rm exp}$, unless the polynomial fit was inadequate. Therefore, this part of the test allows us to check the accuracy of the error estimation of the Stokes parameters.

Even in the case that $P_{\rm res}$ and $P_{\rm exp}$ fit, some data may lie outside of the expected distribution. These discrepant points may be identified easily plotting both $P_{\rm res}$ and $P_{\rm exp}$, as we have done in Figures 1, 4, and 7 in the main text. The $P_{\rm exp}$, which are plotted in these figures as a dotted line, are also the estimated errors of the $P_{\rm res}$. To search for spectral regions that are suitable for having their own polarization different from that of the continuum, we simply look at these figures for points with $P_{\rm res} > 2P_{\rm exp}$. Once these points are found, we test if they are significantly distant from the expected distribution using an upper-tail Student's t-test for the mean of those data and the expected mean polarization at the same range of wavelengths. If the distribution data differ significantly, then it is necessary to compute the probability that such a result or worse is found by chance in the whole set of data.

REFERENCES

Antonucci, R. 1992, in Testing the AGN Paradigm, ed. S. Holt, S. Neff, & M. Urry (New York: AIP), 486
Antonucci, R. R. J., & Miller, J. S. 1985, ApJ, 297, 621
Björnsson, C. I. 1985, MNRAS, 216, 241
Björnsson, C. I., & Blumenthal, G. R. 1982, ApJ, 259, 805
Brown, L. M. J., et al. 1989, ApJ, 340, 129
Cimatti, A., di Serego Alighieri, S., Fosbury, R. A. E., Salvati, M., & Taylor, D. 1993, MNRAS, in press
Courvoisier, T. J.-L., Robson, E. I. Blecha, A., Bonchet, P., Hughes, D. H., Krisciunas, K., & Schwarz, H. E. 1988, Nature, 335, 330
Cruz-Gonzalez, I., & Uchra, J. P. 1984, AJ, 89, 441
De Diego, J. A., Pérez, E., Kidger, M. R., & Takalo, L. O. 1992, ApJ, 396, L19 (Paper I)
Goodrich, R. W. 1989a, ApJ, 340, 190
———. 1989b, ApJ, 342, 224
Goodrich, R. W., & Miller, J. S. 1988, ApJ, 331, 332
Impey, C. D., Malkan, M. A., & Tapia, S. 1989, ApJ, 347, 96
Jackson, N. 1992, in Proc. 33d Herstmonceux Conference (Cambridge), in press
Jackson, N., & Tadhunter, C. N. 1993, in preparation
Kidger, M. R., & de Diego, J. A. 1992, A&AS, 93, 1
Kidger, M. R., de Diego, J. A., Takalo, L. O., Sillanpää, A., & Okyudo, M. 1993, ApJ, 407, L1
Martin, P. G. 1974, ApJ, 187, 461
Martin, P. G. 1985 in Active Galactic Nuclei, ed. J. E. Dyson (Manchester: Manchester Univ. Press), 194
McLean, I. S., Aspin, C., Heathcote, S. R., & McCaughrean, J. 1983, Nature, 304, 609
Miller, J. S., & Antonucci, R. R. J. 1983, ApJ, 271, L7
Miller, J. S., & Goodrich, R. 1990, ApJ, 355, 456
Nordsieck, K. H. 1976, ApJ, 209, 653
Puschell, J. J., Jones, T. W., Phillips, A. C., Rudnick, L., Simpson, E., Sitko, M. L., Stein, W. A., & Monetti, A. 1983, ApJ, 265, 625
Rudy, R. J., & Schmidt, G. D. 1988, ApJ, 331, 325
Schramm, K.-J., et al. 1993, A&A, in press
Serkowski, K., Mathewson, D. S., & Ford, V. L. 1975, ApJ, 196, 261
Smith, P. S., Balonek, T. J., Heckert, P. A., & Elston, R. 1986, ApJ, 305, 485
Smith, P. S., Elston, R., & Balonek, T. J. 1986, in Continuum Emission in Active Galactic Nuclei, ed. M. L. Sitko (Tucson: Kitt Peak National Obs.), 171
Takalo, L. O., Kidger, M. R., de Diego, J. A., Sillanpää, A., & Nilsson, K. 1992a, AJ, 104, 40
Takalo, L. O., Sillanpää, A., Nilsson, K., Kidger, M., de Diego, J. A., & Pirola, V. 1992b, A&AS, 94, 37
Valtaoja, L., Valtaoja, E., Shakhovskoy, N. M., Efimov, Yu. S., Takalo, L. O., Sillanpää, A., Tornikoski, M., Kidger, M., & de Diego, J. A. 1991, AJ, 102, 1946
Wills, B. J., Netzer, H., & Wills, D. 1985, ApJ, 288, 94